Modeling the similarity and the potential of toluene and moisture buffering capacities of hemp concrete on IAQ and thermal comfort

Anh Dung Tran Le, Jianshun S. Zhang, Zhenlei Liu, Driss Samri, Thierry Langlet

Modeling the similarity and the potential of toluene and moisture buffering capacities of hemp concrete on IAQ and thermal comfort

Anh Dung TRAN LE[1]*, Jianshun S ZHANG[2], Zhenlei LIU[2], Driss SAMRI[3], Thierry LANGLET[1]

[1]Laboratoire des Technologies Innovantes, EA 3899 – Université de Picardie Jules Verne, IUT Amiens, Avenue des Facultés – Le Bailly, 80025 Amiens Cedex 1, France

[2]Department of Mechanical and Aerospace Engineering, Syracuse University, 263 Link Hall, Syracuse University, Syracuse, NY 13244 U.S.A

[3]Centre Scientifique et Technique du Bâtiment (CSTB), 24 rue Joseph Fourier 38400 Saint-Martin-D'Hères, France

anh.dung.tran.le@u-picardie.fr

ABSTRACT

Controlling and understanding indoor humidity and pollutants can help reduce the risk of health concerns. The experimental results suggested that there is a similarity relationship between water vapor and Volatile Organic Compounds (VOC) in diffusion through porous media. In this paper, the similarity between the moisture and pollutant transport and storage coefficients of porous building materials has been clearly established and explained. In addition, two similarity coefficients have been defined for VOC storage and diffusion to estimate the VOC properties from the moisture properties of the same material. A coupled hygric-pollutant (VOC) model which can be used to simulate VOC and hygric behavior of building materials under dynamic conditions is presented. The model which is implemented in the environment SPARK (Simulation Problem Analysis and Research Kernel) suited to complex problems using finite difference technique with an implicit scheme, has been validated with the

experimental data. It is then applied to study the effect of toluene and moisture buffering capacities of a hemp concrete wall on indoor toluene concentration and relative humidity (RH). Hemp concrete was chosen in this study because it is an environmentally-friendly material that is used more and more in building construction. The toluene (TOL, selected VOC for this study) transport and storage properties obtained from hygrique properties of hemp concrete based on the assumption of the similarity between toluene and moisture transport have been modeled and investigated. At the room level, the results obtained show that taking into account the sorption capacity toward moisture and toluene has a significant effect on indoor RH and IAQ because hemp concrete contributes to dampen indoor RH and toluene variations. The numerical model presented is very useful for the building design optimization and can be used for a fast estimation of indoor pollution and hygrothermal conditions in building.

Keywords: Hemp concrete, toluene buffering capacity, moisture buffering capacity, similarity, Indoor Air Quality, modeling ,VOC, moisture

1. Introduction

The means for keeping the indoor relative humidity (RH) and pollutant concentration below a threshold level of interests are necessary and essential to improving building performance in terms of indoor air quality (IAQ), energy performance and durability of building materials. For evaluating the indoor air quality and thermal comfort, concentrations of pollutants such as VOC, indoor temperature and relative humidity in building are the most important factors. It has been shown that one of passive ways to keep the variation in RH between threshold levels in order to save energy and improve the thermal comfort is the use of the moisture buffering capacity of materials (including the building envelope as well as interior objects) (Hameury 2005; Olalekan and Simonson 2006; Woloszyn et al 2009, Tran Le et al 2010, Shea et al 2013, Maalouf et al 2014, Samri et al 2014, Tran Le et al 2016, Moujalled et al 2018). The reduction of indoor VOC through adsorption processes is an important research objective due to its potential to provide improved quality of life for individuals in exposed spaces (Maskell et al 2015, Da Silva et al 2016, Hunter-Sellars et al 2020). Formaldehyde sorption/ desorption process of gypsum boards has been carried out by Matthews et al (1987) and showed it has a significant storage capacity and influences significantly the formaldehyde concentration. The experimental data and semi-empirical models describing the sorption of organic gases in a simulated indoor residential environment (a 50 m^3 room finished with painted wallboard, carpet and cushion, draperies and furnishings) have been carried out by Singer et al (2004). The results showed that the

sorption appears to be a relevant indoor process and that sorption processes on typical residential surfaces can influence gas-phase concentrations on the same scale as ventilation. The contributions from several consumer goods and building materials (gypsum board, ceiling tiles, furniture and carpet) to the overall formaldehyde concentration were investigated in climate-controlled chamber experiments by Gunschera et al (2013). The results showed that the formaldehyde concentration in real indoor air will always be influenced by multiple parameters and cannot be simply calculated from the area-specific emission rate of a building material under consideration of loading rate and air exchange rate as usually done.

The use of vegetable particles (such as hemp shives, flax shives, straw bales, etc.) as building material aggregates is an interesting solution as they are eco-friendly materials and have low embodied energy. Among these vegetable particles, hemp shives have been extensively studied in many researches (Li et al. 2017, Gourlay et al. 2017, Amziane et al. 2017, Lagouin et al 2019, Adamová et al 2019, Viel et al 2019, Aït Oumeziane et al 2020). Hemp shives can be used as particle boards, biodegradable plastics, building materials for thermal and acoustic insulation products (Li et al, 2013, Pantawee et al 2017), etc. Regarding the emissions of bacteria and volatile organic compounds (VOCs), the experimental results showed that they are negligible (Koivula et al 2005, Adamová et al 2019). Hemp concrete which is one of these materials is more and more recommended by the eco-builders for its low environmental impact. The physical properties (thermal conductivity, heat capacity, sorption isotherm, water vapor permeability, etc.) of hemp concrete have been measured by many authors (Collet et al. 2008, Walker and Pavia 2014, Lelievre 2015, Rahim et al. 2015, Colinart et al 2017, Promis et al 2019) showing that this material presents high moisture buffering capacity and a good compromise between insulation and inertia materials. Therefore, hemp concrete is chosen for this study. It is noted that the composition and manufacturing have a significant impact on hygrothermal properties and anisotropie of hemp concrete (Nguyen et al 2010, Magniont et al 2012, Pierre et al 2014, Williams et al 2017, Tran Le et al 2019). Up to date, most studies focus on hygrothermal behavior and mechanical performance of bio-based materials. Although the study of pollutant behavior (VOCs) of bio-based materials is very important as the building materials represent an important part of indoor environments (hygrothermal comfort and IAQ).

Regarding volatile organic compound (VOC), the experimental studies showed that there is a similarity between moisture and VOC diffusion through porous media (Salonvaara et al 2006, Xu et al 2009, Rode et al 2020). Note that the diffusion and sorption of VOC and water vapor in building

materials would be related to physical and chemical properties. Rode et al (2020) showed that the VOC diffusivity in air at reference temperature varies with the molar mass of the VOC and the heavier VOC has a lower diffusivity in free air than the one of water vapor. Da Silva et al (2016) showed that the adsorption/desorption characteristics are related to material microstructure and polarity of the VOCs. Therefore, the difference in physical properties (size, molar mass, polarity, etc.) would play a role in the similar behavior between VOCs and water vapor which needs to be further investigated. The tests with gypsum wallboard, oriented strand board and silicate calcium using a dual chamber experimental system showed this similarity can be used to estimate the VOC diffusion coefficient if the water vapor diffusivity is known for the same material based on the conventional dry cup method (Salonvaara et al 2006, Xu et al 2009). Compared to the previous study of Xu et al (2009), the similarities between VOC and moisture transport in building materials have been extended for non-isothermal problems in the framework of Annex 68 (Rode et al 2020). The experimental results obtained by Gunschera et al (2013) have revealed that the formaldehyde concentration in real indoor air can only be explained accurately when taking into account multiple parameters such as adsorption/desorption as well as diffusion inside material.

The literature review showed that there is lack of a comprehensible and validated model to study the hygric and pollutant behavior of bio-based materials. Therefore, to address this lack, a coupled hygric and VOC transport simulation model has been presented and validated in this paper. In addition, the purpose of this paper is to model the similarities between VOC and moisture transport properties and to show the potential of VOC and moisture buffering capacity of hemp concrete to improve IAQ and thermal comfort. The potential of buffering capacity of hygroscopic material can be explaned by the fact they can adsorb VOC/moisture from the ambient air when the indoor VOC/humidity increases, and release VOC/moisture to the ambient air when the VOC/humidity decreases.The toluene (TOL) was selected as reference VOCs in this study because it is a typical indoor VOC and not water soluble.

2. Coupled moisture, air and pollutant transport model

A coupled hygric and pollutant simulation model presented in Figure 1 has been developed to study the similarity between moisture and pollutant behavior of porous building materials. The model includes equations that describe: moisture and VOC diffusion, moisture and VOC sorption, impact of RH and T on moisture and VOC diffusion/sorption, boundary condition between indoor/outdoor air and building envelope surfaces, etc. In this section, the similarity between the moisture and VOC transport and

storage coefficients of building materials will be established and explained based on the following accepted assumptions:

- Transport of water vapor in building materials is modelled analogously to the transport of VOC.
- Sorption of water vapor is described by the sorption isotherm curve (due to its multilayer adsorption) while it is modelled by the partition coefficient for VOC because it is generally considered as monolayer adsorption.

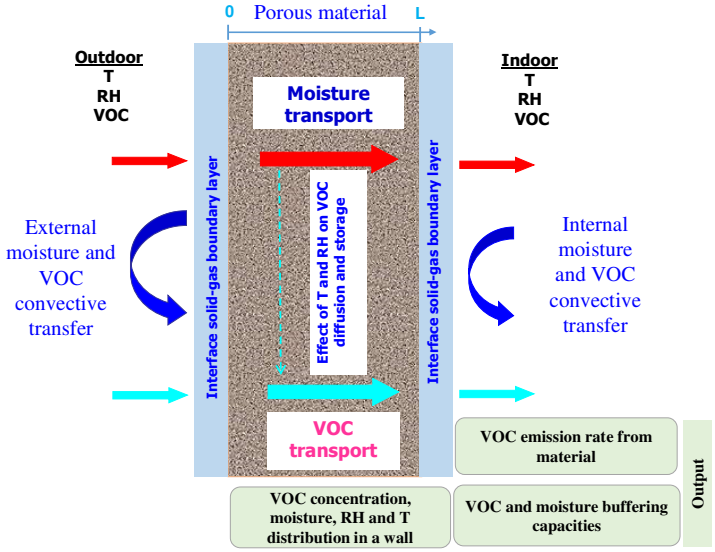

Figure 1: Schematic of coupled moisture and VOC transport model in a wall

2.1 Similarity of pollutants and moisture transport models

In this article, the VOC and moisture diffusion models which take into account the effect of moisture content/RH in building materials on VOC transport are presented. To establish the similarity between the VOC and moisture diffusion models, only concentration gradient of VOC or moisture is assumed to be driving force in the material. It is important to note that the chemical reactions are neglected in this work.

For a dry material with homogeneous diffusivity, the VOC mass transport within the wall can be described by the one-dimensional diffusion (Yang et al 2001, Huang and Haghighat 2002, Zhang 2005):

$$\frac{\partial C_{m,VOC}}{\partial t} = \frac{\partial}{\partial x}\left(D_{m,VOC} \frac{\partial C_{m,VOC}}{\partial x} \right) \quad (1)$$

Where $C_{m,VOC}$ is VOC concentration in the material (kg/m^3), $D_{m,VOC}$ is diffusion coefficient of the VOC in the material (m²/s), x is abscissa (m) and t is time (s). Here, in the developed numerical model,

the $D_{m,VOC}$ is a function of relative humidity/moisture in the material (if the data is available) while the dependence of $D_{m,VOC}$ on pollutants concentration is neglected as generally accepted under low VOC concentration condition.

There is an equilibrium which exists between the concentration of VOC in a material ($C_{m,VOC}$) and the concentration in air ($C_{a,VOC}$), which is defined by the partition coefficient $K_{m,VOC}$:

$$C_{m,VOC} = K_{m,VOC}.C_{a,VOC} \tag{2}$$

The diffusion coefficient of VOC in the material ($D_{m,VOC}$) can be determined from the VOC diffusion coefficient in the free air (D_{VOC}^{air}) and diffusion resistance factor (μ_{VOC}) of VOC (Xu et al 2009):

$$D_{m,VOC} = \frac{D_{VOC}^{air}}{\mu_{VOC} K_{m,VOC}} \tag{3}$$

At the material-air interface, we assume an instantaneous equilibrium between VOC concentration (kg/m^3) in the air near material surface ($C_{a,VOC,s}$) and the one in the surface layer ($C_{m,VOC,s}$):

$$C_{m,VOC,s} = K_{m,VOC}.C_{a,VOC,s} \tag{4}$$

With the following boundary conditions applied respectively for the external (x=0) and internal (x=L) surfaces of the wall:

$$-\left(D_{m,VOC} \frac{\partial C_{m,VOC}}{\partial x} \right)_{x=0,e} = h_{m,\mathrm{VOC},e} \left(C_{a,\mathrm{VOC},e} - C_{a,VOC,s,e} \right) \tag{5}$$

$$-\left(D_{m,VOC} \frac{\partial C_{m,VOC}}{\partial x} \right)_{x=L,i} = h_{m,\mathrm{VOC},i} \left(C_{a,VOC,s,i} - C_{a,\mathrm{VOC},i} \right) \tag{6}$$

Where $C_{a,VOC,i}$ and $C_{a,VOC,e}$ are VOC concentration in the room air and outside (kg/m^3); $C_{a,VOC,s,i}$ and $C_{a,VOC,s,e}$ are VOC concentrations in the air near internal and external surfaces (kg/m^3); $h_{m,VOC,e}$ and $h_{m,VOC,i}$ are convective VOC transfer coefficients (m/s) for the external and internal surfaces, respectively.

Concerning the moisture transport model, the moisture transport within the wall can be described by the one-dimensional diffusion for using moisture content in material as driving force (Philip and De Vries 1957):

$$\frac{\partial \theta}{\partial t} = \frac{\partial}{\partial x}\left(D_{m,\mathrm{wv}} \frac{\partial \theta}{\partial x} \right) \tag{7}$$

Where θ is moisture volumetric content in the material (m^3 of water/m^3 of material), $D_{m,wv}$ is diffusion coefficient of the moisture in the material (m^2/s) which is defined by (Philip and De Vries 1957, Mendes 1997):

$$D_{m,\mathrm{wv}} = \delta_{wv} \frac{P_{v,sat}}{\rho_w} \frac{1}{\partial\theta/\partial RH} = \frac{\delta_{wv}^{air}}{\mu_{wv}} \frac{P_{v,sat}}{\rho_w} \frac{1}{\partial\theta/\partial RH} \tag{8}$$

$\partial\theta/\partial RH$ is the slope of the sorption isotherm curve which designates the relationship between the moisture content and the relative humidity (RH) at a fixed temperature, δ_{wv} is water vapor permeability of material (kg/(m.s.Pa)), ρ_w is density of water (kg/m^3), $P_{v,sat}$ saturation pressure of water vapor (Pa), μ_{wv} the vapor diffusion resistance factor and δ_{wv}^{a} is water vapor permeability of still air ((kg/(m.s.Pa)) which can be determined from D_{wv}^{air} (water vapor diffusion coefficient in the free air, m^2/s), temperature and the gas constant for water vapor (R_v= 461.5 J/(kg·K)):

$$\delta_{wv}^{a} = \frac{D_{wv}^{air}}{R_v T} \tag{9}$$

By replacing (9) in (8) we have:

$$D_{m,\mathrm{wv}} = \frac{D_{wv}^{air}}{\mu_{wv} \frac{\rho_w R_v T}{P_{v,sat}} \frac{\partial\theta}{\partial RH}} = \frac{D_{wv}^{air}}{\mu_{wv} K_{m,wv}} \tag{10}$$

As with the VOC, by identifying two equations (3) and (10), the coefficient $K_{m,wv}$ introduced in (10) is the "partition coefficient" for water vapor, which is similar to $K_{m,VOC}$ in (3) for VOC and can be calculated as following:

$$K_{m,wv} = \frac{\rho_w R_v T}{P_{v,sat}} \frac{\partial\theta}{\partial RH} \tag{11}$$

Note that the partition coefficient ($K_{m,wv}$) for water vapor can be calculated by relating gradients of the absorbed moisture content mass by volume of material, to gradients of the humidity of air by volume of the pores at equilibrium condition. Using this definition to calculate $K_{m,wv}$, the same result was obtained (Rode et al 2020).

Concerning the sorption isotherm, in this article, the Guggenheim-Anderson-deBoer (GAB) model (Timmermann 2003) which is extended from Langmuir and BET theories (Langmuir 1918, Brunauer et al 1938) of physical adsorption, is used to describe the sorption curve. Using the GAB model has many advantages such as having a viable theoretical background and giving a good description of the sorption behavior of hygroscopic material (Andrade et al 2010). The GAB model can be written as follows:

$$w = \frac{w_m C_{GAB} K_{GAB} RH}{\left(1 - K_{GAB} RH\right)\left(1 + K_{GAB} C_{GAB} RH - K_{GAB} RH\right)} \tag{12}$$

Where RH is relative humidity, w is the moisture content (kg of water/kg of material), w_m is the monolayer moisture content value, C_{GAB} and K_{GAB} are energy constants of GAB model.

At the material-air interface, we assume an instantaneous equilibrium between water vapor concentration (kg/m^3) in the air near material surface ($C_{a,wv,s}$) and the one in the surface layer ($C_{m,wv,s}$), which is determined by the sorption isotherm curve. The following boundary conditions applied to water vapor, respectively for the external (x=0) and internal (x=L) surfaces of the wall:

$$-\left(\rho_w D_{m,wv} \frac{\partial \theta}{\partial x}\right)_{x=0,e} = h_{m,\mathrm{wv},e}\left(C_{a,\mathrm{wv},e} - C_{a,wv,s,e}\right) \tag{13}$$

$$-\left(\rho_w D_{m,wv} \frac{\partial \theta}{\partial x}\right)_{x=L,i} = h_{m,\mathrm{wv},i}\left(C_{a,wv,s,i} - C_{a,\mathrm{wv},i}\right) \tag{14}$$

Where $C_{a,wv,i}$ and $C_{a,wv,e}$ are water vapor concentrations in the room air and outside (kg/m^3), and $h_{m,wv,e}$ and $h_{m,wv,i}$ are convective water vapor transfer coefficients (m/s) for the external and internal surfaces.

The mass transfer coefficient may be measured directly or indirectly using the naphthalene sublimation technique or from published heat transfer coefficients or correlations using the so-called heat and mass transfer analogy (Axley 1991). The convection average mass transfer coefficient strongly depends upon the characteristics of the airflow at the material surface. These correlations relate the Sherwood number (Sh), to the Rayleigh (Ra) and Schmidt (Sc) numbers in the case of natural convection, and to the Reynolds (Re) and Schmidt (Sc) numbers in the case of forced convection

(Blondeau et al 2008). The convective mass transfer coefficient for VOC and water vapor (WV) ($h_{m,VOC}$, $h_{m,wv}$) can be calculated by the following equations (White 1991, Axley 1991, Blondeau et al 2008):

$$Sh = 0.037 Sc^{\frac{1}{3}} \mathrm{Re}^{\frac{4}{5}} \text{ for turbulent flow} \quad (15)$$

$$Sh = 0.664 Sc^{\frac{1}{3}} \mathrm{Re}^{\frac{1}{2}} \text{ for laminar flow} \quad (16)$$

$$Sh = \frac{h_m L}{D^{air}} \quad (17)$$

$$Sc = \frac{\upsilon}{D^{air}} \quad (18)$$

where, Sh is Sherwood number, Sc is Schmidt number, h_m is the convective mass transfer coefficient (m/s), L is the characteristic length (m), D^{air} is diffusion coefficient of VOC/water vapor in air (m^2/s), υ is kinematic viscosity of air at 23 °C, which equals 1.544 $x10^{-5}$ m^2/s (Cengel and Ghajar 2010). From equations (15) to (18), we can establish the similarity relationship between $h_{m,wv}$ and $h_{m,VOC}$. Note that, because of the same sample and the same air flow field in the airtight chamber as the same test condition for the combined moisture and VOC study, the same Reynolds number can be considered, and we have the following formula:

$$\frac{h_{m,\mathrm{wv}}}{h_{m,\mathrm{VOC}}} = \left(\frac{D_{wv}^{air}}{D_{VOC}^{air}} \right)^{2/3} \quad (19)$$

Equation (19) permits to determine the convective mass transfer coefficient of VOC ($h_{m,VOC}$) from the convective mass transfer coefficient of water vapor $h_{m,wv}$ (or inversely) using the diffusion coefficients of VOC and water vapor in the air, respectively.

2.2 Model for a room

In order to model the indoor VOC and humidity in the room, we used a nodal method, which considers the room as a perfectly mixed zone characterized by a moisture and pollutant concentrations. Nodal method involves equations for moisture/pollutant (VOC) mass balance and equations describing mass transfer through the walls, additional convection between inside wall surfaces and room ambiance.

The moisture/VOC level in the room is determined by the moisture/VOC transfer from interior surfaces, moisture/VOC production rate and the gains or losses due to air infiltration, natural and mechanical ventilation, sources due to habitants of room as well as the moisture/VOC buffering capacity of other room elements (such as furniture, bookshelf, woolen carpet, etc.). This yields to the following mass balance equation for water vapor/VOC:

$$V\frac{\partial C_{a,i}}{\partial t} = Q\left(C_{a,o} - C_{a,i}\right) + \sum A.h_{m,i}\left(C_{as,i} - C_{a,i}\right) + G \quad (20)$$

Where $C_{a,i}$ is the VOC/water vapor concentration at time t (kg/m^3); $C_{a,o}$ is outdoor ventilation air; V is volume space (m^3); the summation symbol represents the sum of moisture/VOC exchanged between indoor air and the exposed area of the material; A is exposed area of the material (m²); Q is the volume air flow rate into (and out) of the room (m^3/s); G is the generation rate of VOC/water vapor in the room (kg/s).

2.3 Numerical solutions and validation

The set of equations describing the model has been solved using the finite difference technique with an implicit scheme. The Simulation Problem Analysis and Research Kernel (SPARK) developed by the Lawrence Berkeley National Laboratory-USA, a simulation environment allowing to solve efficiently differential equation systems has been used to solve this set of equations (Sowell and Haves 2001, Wurtz et al 2006, Mendonça et al 2006, Tran Le et al 2009, Tran Le et al 2016).

Note that the equations contain several parameters that are themselves function of the state variables. The special interests of the developed model in this paper are the dependencies of moisture transport coefficient, pollutant diffusion coefficient, partial coefficient, etc. upon the relative humidity and temperature can be taken into account if the data is available. This makes it possible to take into account of the effect of T and RH on pollutant and hygrothermal behavior of building materials into the model.

This section concerns the validation of the developed model by comparing the numerical results with experimental ones obtained using the dynamic dual chamber method developed by Xu and Zhang (2009; 2011). The two stainless steel chambers which have the dimension of 0.35 m x 0.35 m x 0.15 m each were partitioned by a test specimen (Figure 2). Each chamber was supplied with inflows under

controlled temperature and relative humidity. Both chambers were supplied with the same airflow rate ($Q=6.58x10^{-2}$ m^3/s) and were placed in the laboratory with constant temperature 23 °C.

Concerning the relative humidity of the inflow for both chambers, it was maintained at threshold level by bubbling the liquid water via a PID (proportional-integral-derivative) control. The temperature and relative humidity of the inflow and outflow for both chambers were recorded continuously by a computer-based data acquisition system.

Regarding VOC, chamber A had a constant VOC injection in the inflow which was supplied by a Dynacalibrator containing a VOC permeation tube maintained at a specific temperature while chamber B had no VOC injection. The VOC concentration in the inflow of chamber A was set at constant, and the concentration in chambers A and B were continuously monitored until they reached a steady state. Concentrations in the outlets of chamber A and B were monitored as C_{Aout} and C_{Bout}. Under well mixed condition, $C_A=C_{Aout}$ and $C_B=C_{Bout}$ and at steady state, C_{Aout} and C_{Bout} were constant. Constant VOC concentration into chamber A (C_{Ain}) was provided by the permeation tube within a dynacalibrator. VOC concentrations (toluene) of the outflows of both chambers were measured by proton transfer reaction mass spectrometry (PTRMS), which was pre-calibrated by the permeation tube under each RH condition because PTRMS measurement might be influenced by RH depending on the property of the specific VOC. Note that, RH and VOC concentration in the inflow of chamber A (C_{Ain} and RH_{Ain}), in chamber B (C_B and RH_B) are used as the input data. The relative humidity and VOC concentration in chamber A (C_A and RH_A) are used for model validation.

Calcium silicate was selected as a reference material for the model validation in this study because of its well-characterized moisture diffusion properties and wide usage as a building insulation material. Besides, calcium silicate is hygroscopic material and clean meaning that it had no VOCs added in the

fabrication. The calcium silicate was cut into a 30.5 cm x 30.5 cm x 1.0 cm, and sealed four edge sides by VOC free tape (resulted in a real exposed area of 0.093 m^2) to prevent VOC diffusion through the edges. The specimen was then placed in a specially prepared steel specimen holder between two chambers, and clamped tightly together. More information about the testing can be fund in Xu and Zhang (2009, 2011). In order to validate the developed models, two tests were used:

- Test for validating the VOC model: VOC concentration (toluene) has been injected (C_{Ain}=383 $\mu g/m^3$) into chamber A while T and RH in both chambers A and B were maintained at 23°C and 50%RH. In the meantime, VOC, RH (C_{Ain} and RH_{Ain}, C_A and RH_A, C_B and RH_B) have been recorded continuously.

- Test for validating the moisture model: the initial RHs in chamber A and B were both 50%. When the test began, the RH of inflow for chamber A was increased to 80% RH while maintaining a constant 50% RH inflow for chamber B, and the changes of RHs in chamber A and B were monitored over time.

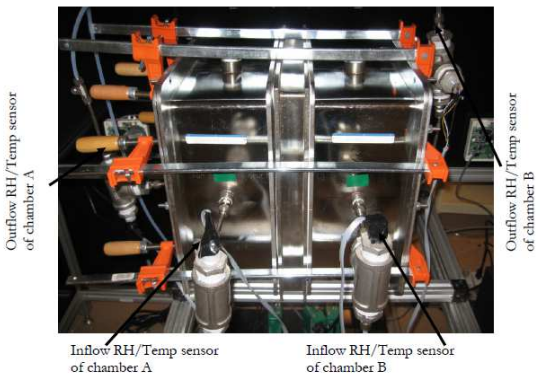

Figure 2.a: Photograph

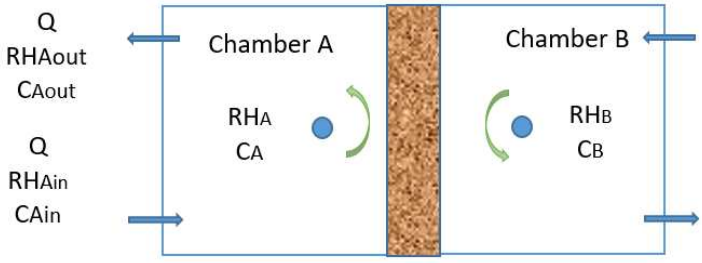

Figure 2.b: Schematic for simulation

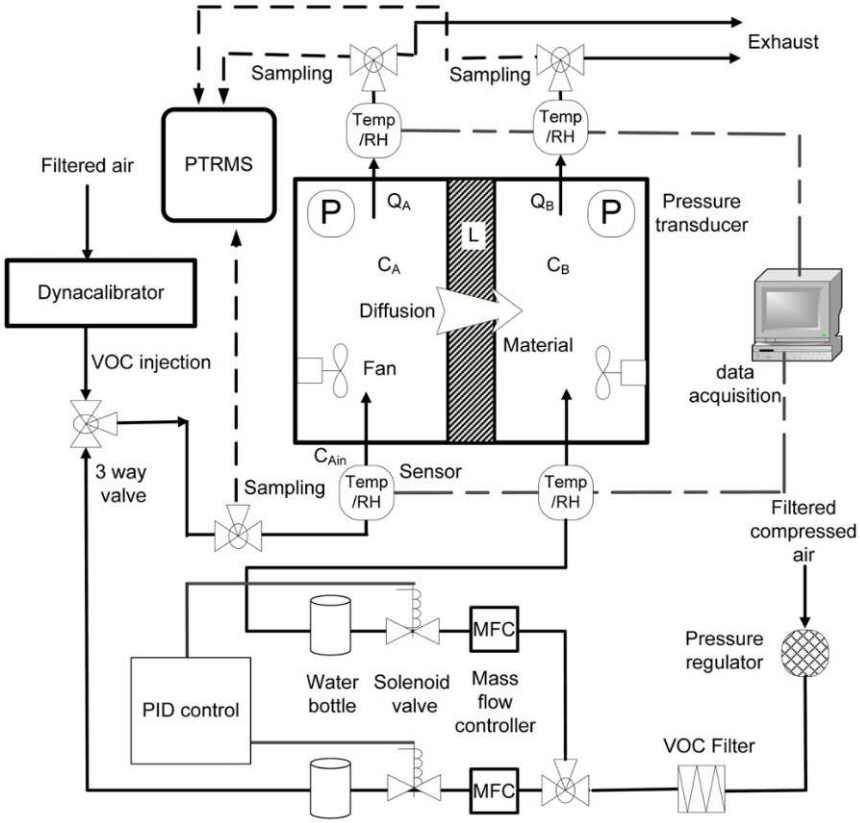

Figure 2.c :Detailed schematic (Xu and Zhang 2011)

Figure 2: Dual chamber system: photograph, detailed schematic (Xu and Zhang, 2011) and test schematic for simulation conditions.

The physical, hygrique and toluene properties of silicate calcium at 50% RH shown in Table 1 and Figure 3 (for sorption isotherm) have been measured by Xu and Zhang (2009) and were used for the model validation. Figure 4 and Figure 5 compare the simulating toluene concentrations and relative humidity in the chamber A. The results show a good agreement between the numerical model and experimental results after the few hours for both pollutant and moisture models. Therefore, the developed model is satisfying to investigate the coupled hygric-pollutant (toluene) behavior of porous building materials. In the next section, the modeling toluene properties from moisture properties of hemp concrete will be presented.

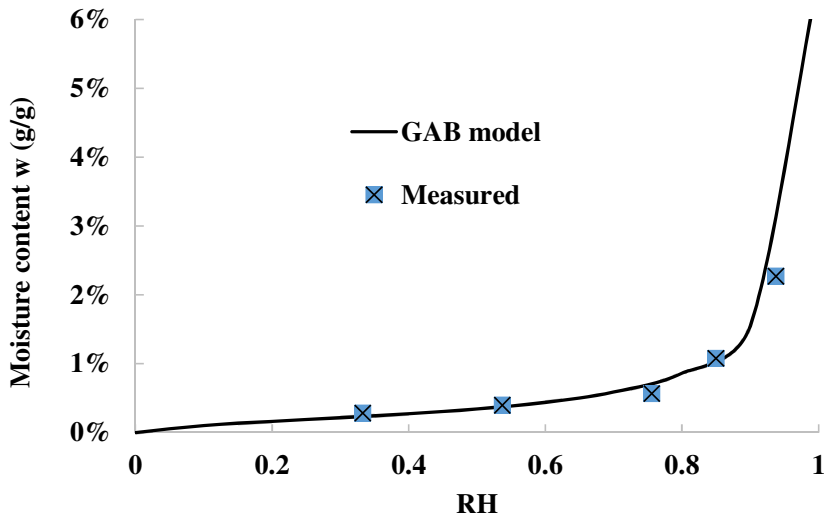

Figure 3: Sorption isotherm of silicate calcium (Xu and Zhang, 2009)

ρ (kg/m^3)	μ_{wv}	μ_{TOL}	$K_{m,TOL}$	$D_{m,TOL}$ (m²/s)	Sorption isotherm (GAB model parameters, R^2=0.99)
843.38	8.71	4.94	133	1.29×10^{-8}	w_m=0.002; C_{GAB}=8; K_{GAB}=0.97

Table 1: Physical, hygric and toluene properties of silicate calcium (SC) for toluene at 50% RH (Xu and Zhang, 2011) and GAB model parameters proposed for SC.

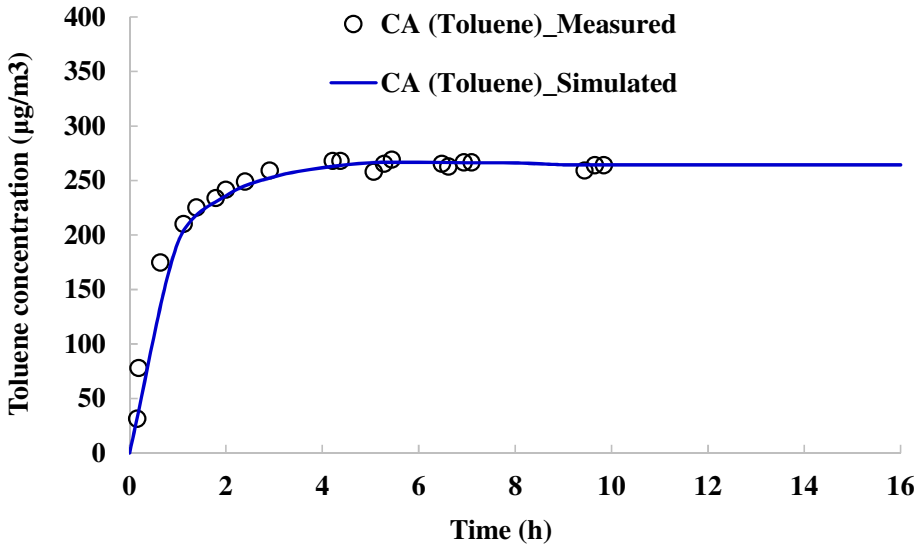

Figure 4: Computed values and measured toluene indoor concentration in chamber A

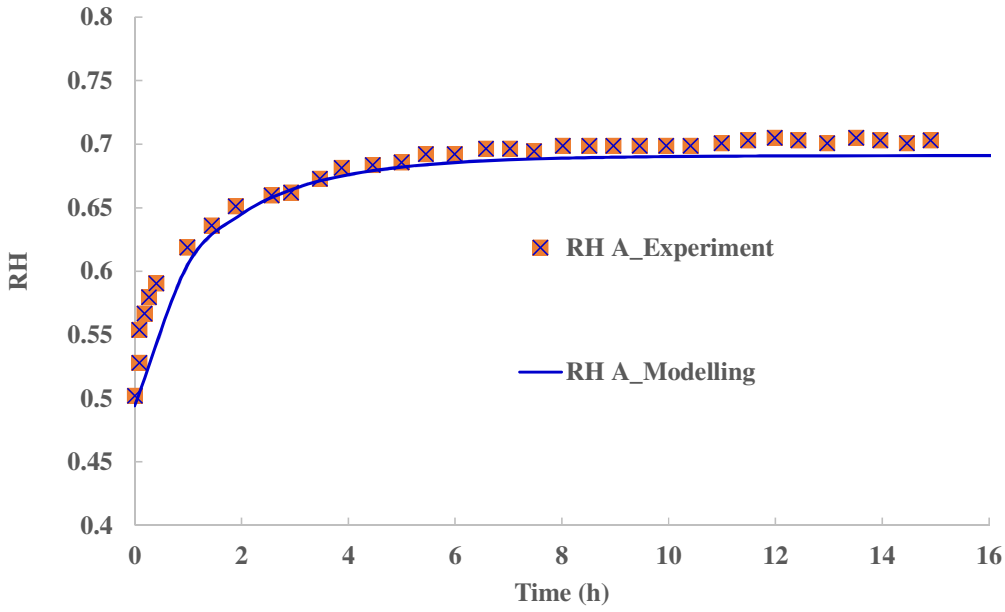

Figure 5: Computed values and measured RH in chamber A

3. Effect of toluene and moisture buffering capacities of hemp concrete wall on indoor relative humidity and toluene concentration

3.1 Modeling toluene properties from moisture properties of hemp concrete

An increased environmental awareness incites to the valorization of plant resources as building materials or incorporating construction processes. One of these building materials is hemp concrete, which has been used widely in the world and extensively studied in many researches. At the building level, it has been proven that the use of hemp concrete can damping the variation indoor RH thank to its moisture buffering capacity (Tran Le et al 2010, Shea et al 2013). Hemp concrete has been selected for this study because it is more and more recommended by the eco-builders for its low environmental impact, excellent moisture buffering capacity and a good thermal insulation (Collet 2008, Samri 2006, Tran Le et al 2010). This article will focus on modeling toluene properties of sprayed hemp concrete which is made of hemp shiv mixed with Tradical PF70 binder for wall application, from the moisture properties experimentally determined in (Collet et al 2013, Lelievre 2015, Colinart et al 2017). The toluene (water insoluble) which is a typical indoor VOC was selected as reference VOCs. Regarding the fact that the calculated mean free path for toluene is 14.3 nm (Xu et al 2009) and the mean pore diameter in hemp concrete is about 780 nm (Collet 2004), the molecular diffusion dominates the mechanism for toluene. Concerning water vapor, its mean free path is 100 nm (Collet 2004), the molecular diffusion is predominant in hemp concrete compared to Knudsen diffusion which is also expected to occur.

Xu et al (2009) proposed the similarity coefficient to correlate the pore diffusion coefficient of VOCs with that of water vapor for hygroscopic moisture conditions. The similarity coefficient for the moisture and VOC diffusion can be determined by:

$$\kappa_{\mu,VOC} = \frac{\mu_{VOC}}{\mu_{wv}} = \frac{D_{VOC}^{air}}{\mu_{wv} D_{m,\mathrm{VOC}} K_{m,VOC}} \tag{21}$$

The partition coefficient of VOC can be determined based on the vapor pressure of the compound for different materials. Based on the data obtained by Bodalal (1999), the following correlation may be used when the material and compound to be studied do not match the data available (Yang et al 2001):

$$K_{m,VOC} = 10600 P^{-0.91} \tag{22}$$

where P is the vapor pressure of the compound in mmHg. By using equation (22) for toluene (P=25.8 mmHg at 23°C), the partition coefficient of toluene $K_{m,TOL}$ for hemp concrete is 550.

The similarity coefficient between toluene and water vapor ($\kappa_{\mu,TOL}$=0.56) which was experimentally determined by Xu et al (2009) is used to estimate the toluene diffusion coefficient for hemp concrete. Table 2 and Figure 6 show the physical properties, vapor diffusion resistance factor and adsorption isotherm of hemp concrete obtained by other authors (Collet et al 2013, Colinart et al, 2017, Lelievre 2015). The results show that hemp concrete is a very porous and hygroscopic material. The calculated values of $\mu_{m,TOL}$ and $D_{m,TOL}$ by equations (21) are shown in Table 3.

Concerning the partition coefficient of water vapor ($K_{m,wv}$), it is calculated by Equation (11) and the result determined at 10% RH is reported in Table 3. Equation (11) shows that $K_{m,wv}$ depends on temperature, relative humidity and the slope of the sorption isotherm of material. We can define the similarity coefficient for the moisture and VOC storage as following:

$$\kappa_{K_{m,VOC}} = \frac{K_{m,VOC}}{K_{m,\mathrm{wv}}} \tag{23}$$

Note that it is very interesting to study the similarity ($K_{m,VOC}$/ $K_{m,wv}$ and $\mu_{m,VOC}$/ $\mu_{m,wv}$ for storage and diffusion properties, respectively) between VOC and moisture transport in building materials. If the similarity is justified and validated by experimental results for other pollutants, the VOC properties can be determined directly from the vapor diffusion resistance factor ($\mu_{m,wv}$) and the slope of the sorption curve in the monolayer sorption range (from 0 to 20% RH, before the beginning of multilayer sorption for hemp concrete case) because the VOCs sorption is generally monolayer in building materials. In this study, the calculated value of $\kappa_{K_{m,TOL}}$ for hemp concrete is 0.38 compared to 0.33 for silicate calcium obtained experimentally by Xu and Zhang (2009).

Dry density (kg/m^3)	Total porosity (%)	Open porosity (%)	μ_{wv}	Sorption isotherm (GAB model parameters)
450	78	66	5	w_m=0.02; C_{GAB}=7; K_{GAB}=0.89

Table 2: Hygric properties of hemp concrete to model toluene properties

μ_{TOL}	μ_{wv}	$K_{m,wv}$	$K_{m,TOL}$	$D_{m,TOL}$ (m²/s)
2.8	5	1434 (at 10% RH)	550	$5.5x10^{-9}$

Table 3: Toluene (TOL) and moisture properties of hemp concrete for the simulation

3.2 Description of studied room and simulation conditions

The studied office is depicted in Figure 7 and has a space area of 5*4 m² and a volume of 50 m^3. To study the impact of moisture and toluene buffering capacities of hemp concrete on the indoor RH and toluene concentration, we consider a total exposed surface area S=25 m^2 of hemp concrete (moisture and toluene interactions between indoor air and building materials are taken into account). The hygric and pollutant properties of hemp concrete presented in Table 2, Table 3 and Figure 6 were used for the simulation. The room temperature is constant and kept at 20°C. The ventilation uses the external conditions in which the outdoor temperature and relative humidity are 20°C and 50 %, respectively. The room is occupied by two persons from 8.00 am to 17.00 pm and the water vapor source is 142 g/h. The air velocity over the wall is 0.15 m/s which is a typical designed value in buidings to ensure thermal comfort of the occupants. The convective mass transfer coefficients for toluene and water vapor ($h_{m,TOL}$ and $h_{m,wv}$) were calculated by the equations (15)-(19).

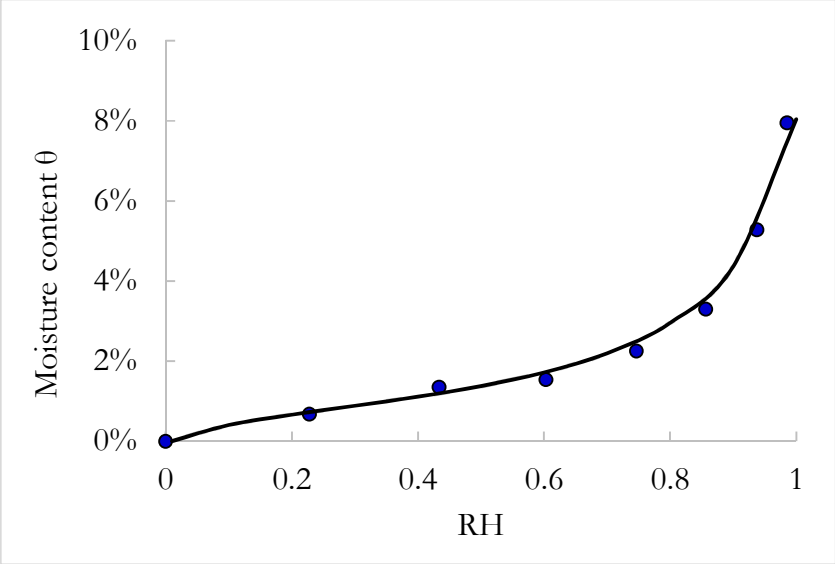

Figure 6: Sorption isotherm of hemp concrete

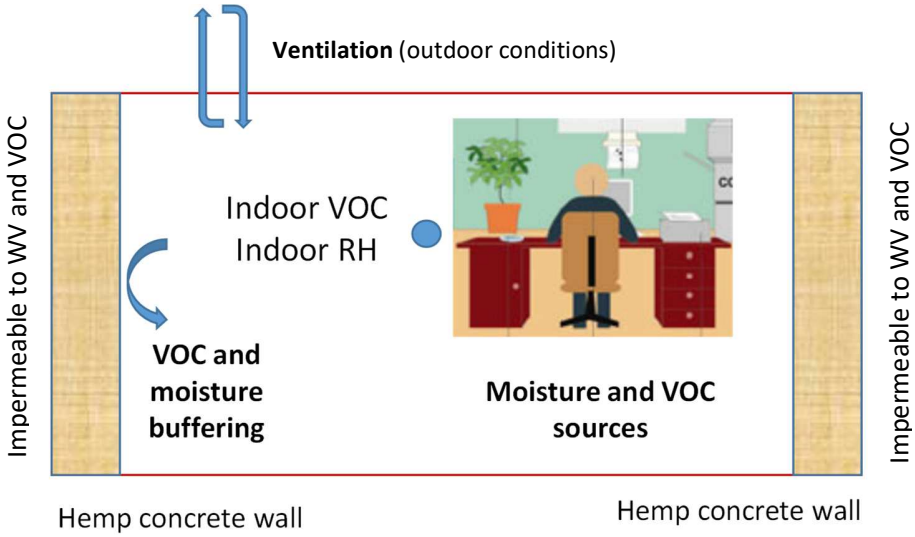

Figure 7: Studied configuration

In this article, an outdoor toluene concentration of 0 mg/m^3 and a ventilation rate of 0.72 ACH (Air Changes per Hour) determined based on the ventilation rate required in the French office buildings are considered. The hemp concrete wall has a thickness of 20 cm and is divided into 25 nodes. The time step is 240s. The only interaction (moisture/ toluene) between the internal exposed surface of hemp concrete wall and indoor air is taken into account and the other faces of the material are considered "well sealed". The initial relative humidity is 60% RH and the initial toluene concentrations C_0 in hemp concrete is 0 (µg/m^3) because it is considered as a clean material. To study the effect of toluene buffering capacity of hemp concrete, a toluene source scheme following is considered: 12 hours of 1000 µg/h followed intermittently 12 hours of 0 µg/h.

In this paper, two models have been considered:

- **Model with buffering capacity (BC** model): Simulation taking into account the moisture and toluene sorption capacities.
- **Model without buffering capacity (Without-BC** model): Simulation neglecting the moisture and toluene sorption capacities.

3.3 Results and dicussion

3.3.1 Impact of toluene and moisture buffering capacities of hemp concrete wall on indoor RH and toluene concentration

The simulated results of the two models with and without toluene -moisture buffering capacity are presented in Figure 8 and Figure 9. In addition, Table 4 presents the analysis results (indoor RH and toluene concentration) obtained from the simulation when the equilibrium state is reached. Figure 8 showed a significant effect of the toluene buffering capacity of hemp concrete on indoor toluene variation. We define a parameter called "*peak reduced factor-PRF*" which is calculated from the indoor concentration with and without buffering capacity (C_0 corresponds to the case without buffering capacity):

$$PRF = \frac{C_0 - C}{C_0} \quad (24)$$

The PRF_{VOC} value allows to quantify the VOC buffering capacity of building materials. Regarding the values of indoor pollutant concentration at the equilibrium state, the maximum values of **BC** and **Without-BC** models are 23.6 and 27.8 μg/m^3, respectively (Table 4) (so a PRF_{TOL} of 15%). Note that PRF_{TOL} value depends on the exposure time. From IAQ analysis and design point of view, it is very interesting to define a parameter that takes into account the concentration reduction and exposure time. Thus, we define an index called "Cumulative Exposure Reduction Factor, ERFc" (unity is %.h)" which is calculated by:

$$\text{ERFc}=\int_0^t PRF dt \quad (25)$$

The ERFc for toluene is 210.5 % for 12 hours exposure in this study. The results reveal that taking into account the toluene sorption capacity in the simulation results in damping the peak of indoor toluene concentration and thus contributes to ameliorate the indoor air quality. Concerning the variation of the indoor relative humidity, it is presented in Figure 9 and Table 4. The results show that the moisture buffering capacity of hemp concrete allows to dampen the indoor relative humidity variation. Numerically, at the equilibrium state, the maximum indoor RH values decrease from 72.5 % to 66.3% RH (a difference of 6.2 % RH and PRF_{RH}=8.6 %) for **Without-BC** and **BC** models, respectively. For indoor humidity, we define a parameter called "*amplitude reduced factor-*RF_a" which is calculated from the amplitude of indoor relative humidity variation with and without moisture buffering capacity (A_0 corresponds to the case without moisture capacity):

$$RF_a = \frac{A_0 - A}{A_0} \quad (26)$$

The RF_a value allows to quantify the hygric buffering capacity of building materials. In addition, the RF_a value of 43.4 % is obtained at peak concentration showing that taking moisture buffering

capacity into account can reduce the indoor RH variation amplitude by 43.4 %.

	Indoor Toluene (µg/m³)			Indoor RH (%)		
	TOL min	TOL max	Amplitude	RH min	RH max	Amplitude
BC model	3.2	23.6	20.4	53.5	66.3	12.8
Without-BC model	0	27.8	27.8	50	72.5	22.5

Table 4: Effect of toluene and moisture buffering capacities of hemp concrete on indoor toluene concentration and RH calculated at the equilibrium state

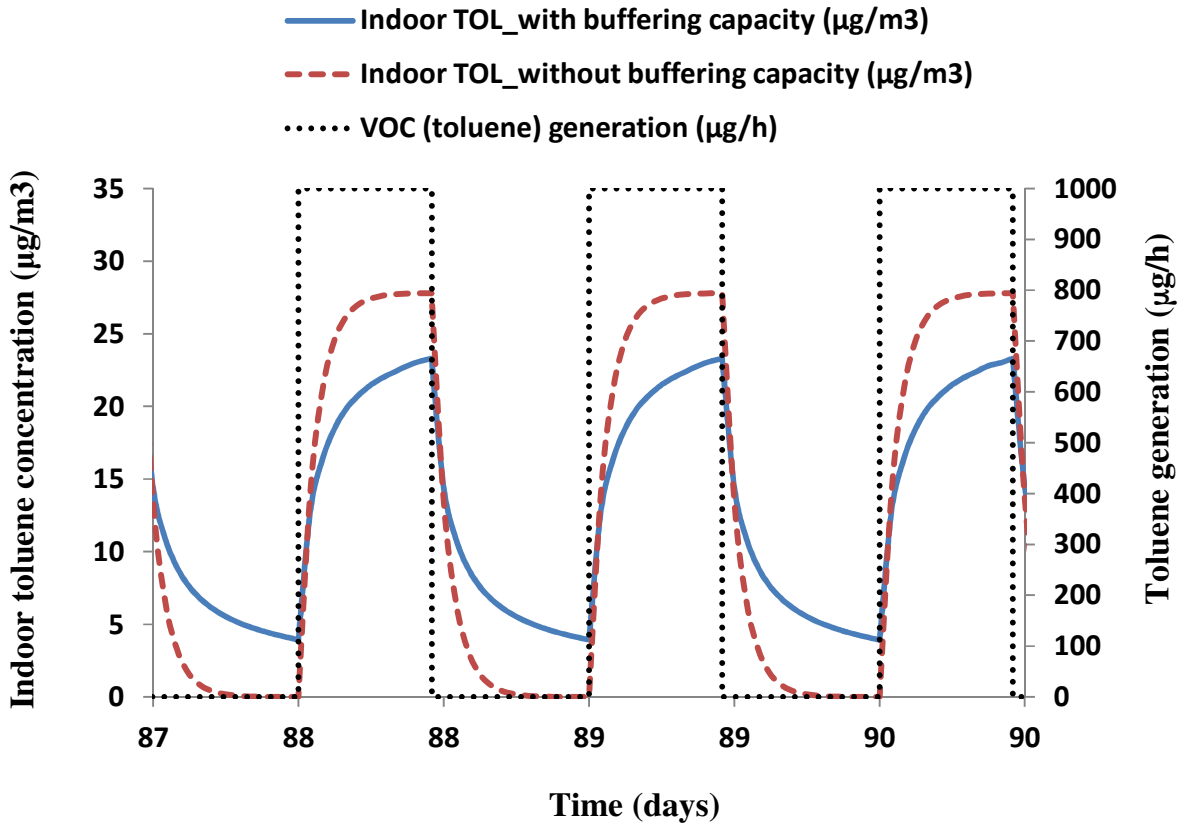

Figure 8: Effect of toluene (TOL) sorption capacity of hemp concrete on indoor toluene concentration

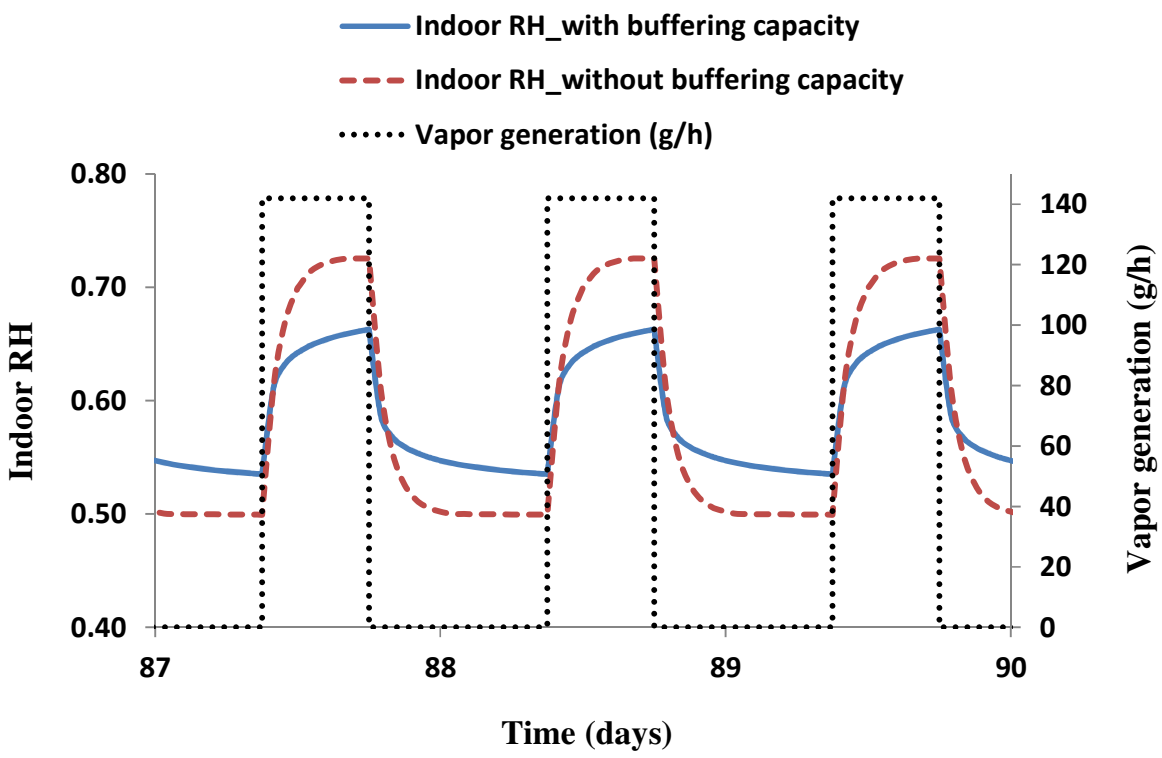

Figure 9: Effect of moisture sorption capacity of hemp concrete on indoor RH

3.3.2 Influence of $D_{m,VOC}$ and $K_{m,VOC}$ on toluene buffering capacity of hemp concrete

It is very important to understand the influences of two key parameters $D_{m,TOL}$ and $K_{m,TOL}$, which have been modeled based on the similarity between toluene and water vapor diffusion in porous material on toluene behavior of hemp concrete. Therefore, a sensibility study of toluene buffering capacity of hemp concrete to its toluene properties has been carried out. In this part, the impact of each individual parameter ($D_{m,TOL}$ or $K_{m,TOL}$) on the resulting indoor toluene concentration parameter while all the other parameters remain the same as those of the reference case has been carried out.

To study the impact of the material-air partition coefficient ($K_{m,TOL}$), we considered the following values: 250; 550 (reference case); 1000; 2500, 5000. The numerical results are presented in Figure 10 and Table 5 and show that $K_{m,TOL}$ has a significant effect on both the indoor toluene concentration and

the decay/growth rate of the concentration curve. It can be seen that during the adsorption period, increasing the $K_{m,TOL}$ increases the toluene adsorption which is then diffuses into material and results in a slower indoor toluene concentration and a higher PRF_{TOL} and $ERF_{c,TOL}$ values. Numerically, during the adsorption period, when $K_{m,VOC}$ increases from 250 to 550 (reference case), 1000, 2500 and 5000, the PRF_{TOL} value increases from 8.8% to 15%, 19.6%, 25.6% and 30.1%, respectively (see Table 5). The observation is reversed during the desorption period.

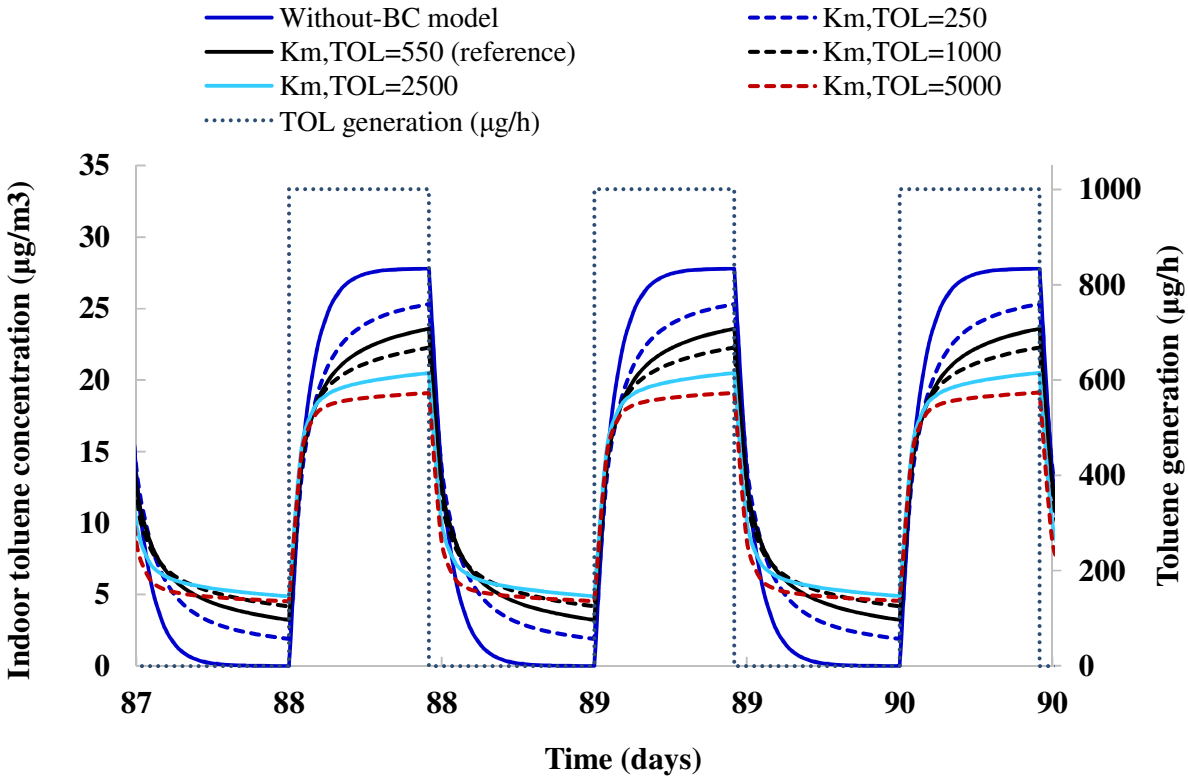

Figure 10: Effect of $K_{m,TOL}$ of hemp concrete on indoor toluene concentration

$K_{m,VOC}$	C_{max} (µg/m³)	C_{min} (µg/m³)	Amplitude (µg/m³)	PRF_{TOL} (%)	$ERF_{c,TOL}$ (%.h)
$K_{m,VOC}$ =5000	19.4	4.6	14.8	30.1	343.0
$K_{m,VOC}$ =2500	20.7	4.9	15.8	25.6	293
$K_{m,VOC}$ =1000	22.3	4.2	18.2	19.6	246.8
$K_{m,VOC}$ =550 (reference)	***23.6***	***3.2***	***20.4***	***15.0***	***210.5***
$K_{m,VOC}$ =250	25.3	1.9	23.4	8.8	149
Without-BC model	27.8	0.0	27.8	0.0	0

Table 5: Impact of $K_{m,TOL}$ of hemp concrete on indoor toluene concentration, amplitude, PRF_{TOL} and $EFR_{C,TOL}$

Concerning the influence of $D_{m,TOL}$ (m²/s), the following values have been used for the simulation: $5.5x10^{-7}$; $5.5x10^{-8}$; $5.5x10^{-9}$ (reference case); $5.5x10^{-10}$ and $5.5x10^{-11}$ (m²/s) which have been denoted by: $100xD_{m,TOL,reference}$; $10xD_{m,TOL,reference}$; $D_{m,TOL,reference}$; $0.1xD_{m,TOL,reference}$ and $0.01xD_{m,TOL,reference}$, respectively (see Figure 11). The numerical results presented in Figure 11 and Table 6 show that the impact of $D_{m,TOL}$ is significant. During the adsorption period, higher $D_{m,TOL}$ results in a lower peak concentration. However, the impact of a change in $D_{m,TOL}$ is insignificant when the $D_{m,TOL}$ value is below $5.5x10^{-11}$ (m²/s) or above $5.5x10^{-8}$ (m²/s). Numerically, when $K_{m,TOL}$ increases from 550 to 1000 (by a factor of 1.8) the PRF_{TOL} increases from 15% to 19.6 % (see Table 5) compared to a value of 22.2% when $D_{m,TOL}$ increases by a factor of 10 ($D_{m,TOL}$ increases from $5.5x10^{-9}$ to $5.5x10^{-8}$ (m²/s)). The results suggest that the toluene buffering capacity of the SC board depends on both $K_{m,TOL}$ and $D_{m,TOL}$ but more sensitive with variation of the material-air partition coefficient ($K_{m,TOL}$).

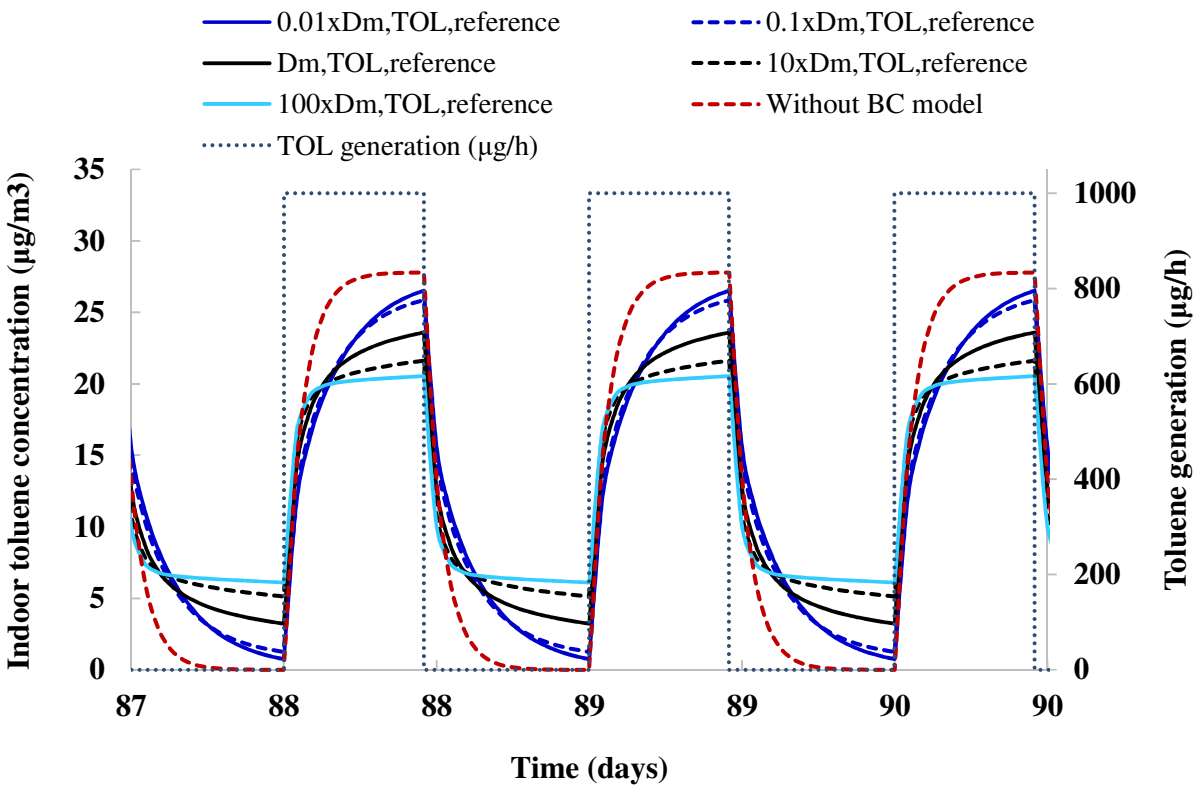

Figure 11: Effect of $D_{m,TOL}$ of hemp concrete on indoor toluene concentration

Cases studied	C_{max} (µg/m³)	C_{min} (µg/m³)	Amplitude (µg/m³)	PRF_{TOL} (%)	$ERF_{c,TOL}$ (%.h)
Without BC model	27.8	0.0	27.8	0.0	0.0
100x $D_{m,TOL,ref}$	20.5	6.1	14.4	26.1	271
10x $D_{m,TOL,ref}$	21.6	5.1	16.5	22.2	252
$D_{m,TOL,ref}$	***23.6***	***3.2***	***20.4***	***15.0***	***210.5***
0.1x $D_{m,TOL,ref}$	25.9	1.3	24.6	6.9	175
0.01x $D_{m,TOL,ref}$	26.5	0.7	25.8	4.6	173.9

Table 6: Impact of $D_{m,TOL}$ of hemp concrete on indoor toluene concentration, amplitude, PRF_{TOL} and $EFR_{C,TOL}$

3.3.3 Impact of exposed surface area (A) and loading ratio on IAQ and indoor RH

The moisture and VOC buffering potential of hemp concrete will be fully utilized when the material is directly exposed to indoor air. In the case that hemp concrete is rendered/ plastered, the internal plaster should have impact on moisture and pollutant buffering capacity of hemp concrete and it is suggested to use the internal plaster which its moisture/VOC penetration depth is greater than their thickness in the system (Latif et al 2015). In addition, regarding the material selection process in building design, it is important to study the effect of exposed surface area (A parameter in equation 20) and the loading ratio (the ratio of the wall surface area to the volume of the room) of hemp concrete on IAQ and hygric performance. Thus, the simulation has been done with different exposed surfaces from 0 to 25 m² (loading ratio from 0 to 0.5) with a step of 5 m². Figure 12, Figure 13, Table 7 and Table 8 show the effect of suface and the loading ratio on indoor toluene, RH and other indices defined previously. It can be seen that the impact of exposed surface (A) is significant and when the loading ration of hemp concrete is increased/decreased, the indoor toluene concentration and RH during the adsorption/desorption period is decreased/increased. Numerically, when the exposed surface decreases from 25 m² to 15 m² (loading ratio decreases from 0.5 to 0.3, so a reduction of 40%), the PRF_{TOL} decreases from 15% to 10% and the PRF_{RH} decreases from 8.6% to 6.4%, respectively. The developed model in this paper is very useful in building design because it can be used to analyze quantitatively the effect of pollutant and moisture buffering capacity of materials which is considered as a solution to improving IAQ as well as hygrothermal performance of buildings.

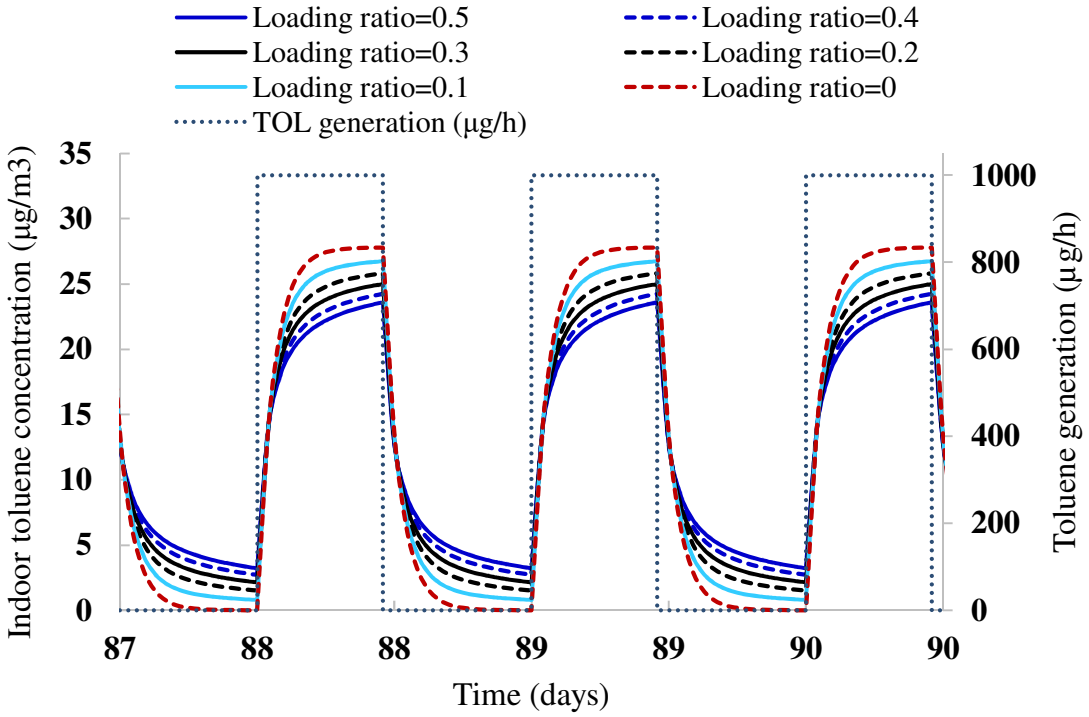

Figure 12: Effect of loading ratio (m^2/m^3) of hemp concrete on indoor toluene concentration

A (m^2)	Loading ratio A/V (m^2/m^3)	C_{max} (µg/m^3)	C_{min} (µg/m^3)	Amplitude (µg/m^3)	PRF_{TOL} (%)	$ERF_{c,TOL}$ (%.h)
0	0.0	27.8	0.0	27.8	0.0	0.0
5	0.1	26.8	0.8	25.9	3.7	56.0
10	0.2	25.8	1.5	24.3	7.1	103.9
15	0.3	25.0	2.1	22.9	10.0	144.5
20	0.4	24.3	2.7	21.6	12.6	179.7
25*	***0.5***	***23.6***	***3.2***	***20.4***	***15.0***	***210.5***

*Reference case

Table 7: Impact of exposed surface (A) and and loading ratio on toluene performance of hemp concrete

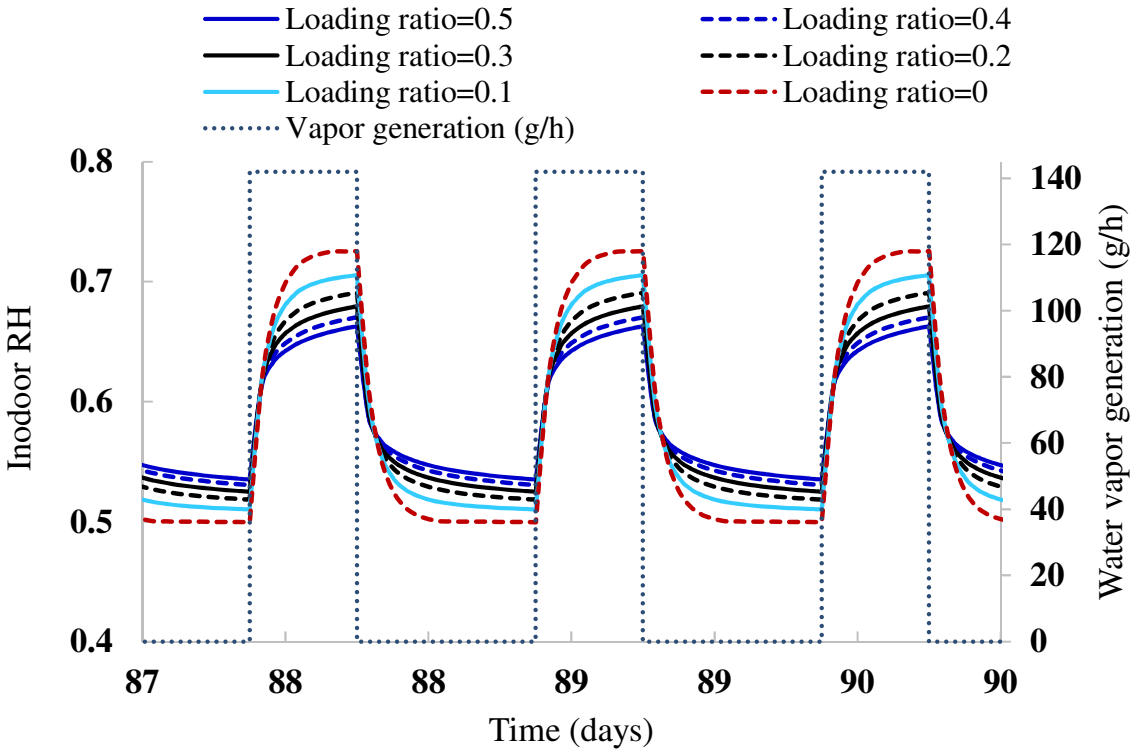

Figure 13: Effect of loading ratio (m^2/m^3) of hemp concrete on indoor RH

A (m^2)	Loading ratio S/V (m^2/m^3)	RH_{max} (%)	RH_{min} (%)	Amplitude (%)	RF_a (%)	PRF_{RH} (%)
0	0.00	72.5	50	22.5	0.0	0.0
5	0.10	70.5	51.0	19.5	13.6	2.8
10	0.20	69.1	51.8	17.3	23.7	4.8
15	0.30	67.9	52.5	15.5	31.6	6.4
20	0.40	67.0	53.0	14.0	38.1	7.6
25*	**0.50**	**66.3**	**53.5**	**12.8**	**43.4**	**8.6**

*Reference case

Table 8: Impact of exposed surface (A) and loading ratio on hygric performance of hemp concrete

4. Conclusion

In this paper, the similarity and the potential of toluene and moisture buffering capacities of hemp

concrete on IAQ and indoor RH has modelled and investigated. Two similarity coefficients $\kappa_{K_m,VOC}$ and $\kappa_{\mu,VOC}$ defined for VOC storage and diffusion have been proposed and can be used to estimate the VOC properties from the vapor diffusion resistance factor ($\mu_{m,wv}$) and the slope of the sorption curve in the monolayer sorption range of the same material. The toluene properties ($K_{m,TOL}$ and $D_{m,TOL}$) were determined from the hygric properties of hemp concrete based on the assumption of the similarity between the moisture and pollutant transport in porous materials. The coupled moisture and pollutant transport simulation model has been established and implemented in SPARK, an object-oriented program suited to complex problems. The numerical model was applied to investigate the effect of the toluene and moisture buffering capacities of hemp concrete on indoor toluene concentration and relative humidity. The results reveal that taking into account the sorption capacity toward moisture and toluene of hemp concrete has a significant impact on indoor RH and IAQ. Numerically, in this case studied, hemp concrete can contribute to dampen 15% the peark of indoor toluene concentration and 43.4% indoor RH variation amplitude. The indices are also proposed to represent the buffering capacity of materials in reducing the occupant's peak exposure (RH and toluene), cumulative exposure to toluene. These definitions are very useful for consideration in future standards that consider buffering as an approach to improving IAQ as well as hygrothermal performance of buildings. Further experiments and analyses are needed to generalize the similarity and the potential of VOC and moisture buffering capacities of bio-based materials for other VOCs with different physical properties (size, molar mass, polarity, etc.). Finally, it is important to note that the developed numerical model allows to study quantitatively the effect of different parameters (D_m, $K_{m,\,VOC}$, exposed surface, loading ratio, etc.) on the IAQ and thermal comfort and can be used to predict the entire VOC emission life of the material to overcome the measurement difficulties.

Acknowledgements

This study was carried out under the program Fulbright/Hauts-de-France which is supported by the Franco-American Fulbright Commission and the Hauts-de-France region, France. Thanks to this financial support, it enabled Dr. Anh Dung TRAN LE to work at the BEESL of Syracuse University, USA for a period of six months. The authors wish to thank them.

The authors wish to thank the editor and reviewers for their constructive and useful comments on the previous version of this article.

Nomenclature

A	Exposed area of the material	m^2
C	Concentration	kg/m^3
$C_{a,o}$	Outdoor ventilation air	kg/m^3
$C_{a,wv,e}$	Water vapor concentrations in the outside	kg/m^3
$C_{a,wv,i}$	Water vapor concentrations in the room air	kg/m^3
$D_{m,VOC}$	Diffusion coefficient of the VOC in the material	$m^2.s^{-1}$
$D_{m,wv}$	Mass transport coefficient associated to a moisture content gradient	$m^2.s^{-1}$
D_{VOC}^{air}	VOC diffusion coefficient in the free air	m^2/s
D_{wv}^{air}	Water vapor diffusion coefficient in the free air	m^2/s
$h_{m,wv,i}$	Convective water vapor transfer coefficient for the internal surface	m/s
$h_{m,wv,e}$	Convective water vapor transfer coefficient for the external surface	m/s
$h_{m,VOC,e}$	Convective VOC transfer coefficient for the external surface	m/s
$h_{m,VOC,i}$	Convective VOC transfer coefficient for the internal surface	m/s
$K_{m,VOC}$	Partition coefficient for VOC	-
$K_{m,wv}$	Partition coefficient for water vapor	-
ERFc	Cumulative Exposure Reduction Factor	%.h

PRF	Peak reduced factor	%
$P_{wv,sat}$	Saturation pressure of water vapor	Pa
Q	Flow rate	m^3/s
RH	Relative humidity	-
R_v	Gas constant for water vapor	J/(kg·K)
T	Temperature	K
t	Time	s
V	Volume space	m^3
w	Moisture content	$kg.kg^{-1}$
w_m	Monolayer moisture content	$kg.kg^{-1}$
x	Abscissa	m
θ	Moisture volumetric content	$m^3 .m^{-3}$
μ_{wv}	Vapor diffusion resistance factor	-
δ_{wv}	Water vapor permeability of material	kg/(m.s.Pa)
δ_{wv}^{a}	Water vapor permeability of still air	kg/(m.s.Pa)
$\kappa_{\mu,VOC}$	Similarity coefficient for the moisture and VOC diffusion	-
$\kappa_{K_m,VOC}$	Similarity coefficient for the moisture and VOC storage	-

Subscripts

e= external

m= material

i= internal

wv= water vapor

VOC= Volatile Organic Compounds

References

Adamová, .T, Hradecký, J., Prajer M. 2019. VOC Emissions from Spruce Strands and Hemp Shive: In Search for a Low Emission Raw Material for Bio-Based Construction Materials. *Materials* (Basel), 12(12):2026. doi: 10.3390/ma12122026. PMID: 31238573; PMCID: PMC6630300.

Aït Oumeziane Y., Collet F., Lanos C., Moujalled B. (2020). Modelling the Hygrothermal Behaviour of Hemp Concrete: From Material to Building. In: Crini G., Lichtfouse E. (eds) Sustainable Agriculture Reviews 42, *Sustainable Agriculture Reviews*, vol 42. Springer, Cham

Amziane, S., Collet, F., Lawrence, M., Magniont, C., Picandet, V., Sonebi, M. 2017. Recommendation of the RILEM TC 236-BBM: characterisation testing of hemp shiv to determine the initial water content, water absorption, dry density, particle size distribution and thermal conductivity, *Mater Struct,* 50, 167.

Andrade, P.R.D., Lemus M.R., Pérez, C.C.E. (2011). Models of sorption isotherms for food: uses and limitations, Vitae 18, 325-334.

Axley J. W. Adsorption Modelling for Building Contaminant Dispersal Analysis', *Indoor Air*, 1 (2) (1991), 147–171.

Blondeau P, Tiffonnet AL, Allard F, Highighat F. Physically based modeling of the material and gaseous contaminant interactions in buildings: models, experimental data and future developments. *Advances in Building Energy Research*, 2008.

Bodalal A. 1999. Fundamental mass transfer modeling of emission of volatile organic compounds from building materials. PhD thesis, Department of Mechanical and Aerospace Engineering, Carleton, University, Canada.

Colinart, T. and Glouannec P. 2017. Temperature dependence of sorption isotherm ofhygroscopic building materials. Part 1: Experimental evidence and modeling, *Energy and Buildings* 139: 360–370.

Collet F.2004. Caractérisation hydrique et thermique de matériaux de génie civil à faibles impacts environnementaux, Thèse de Doctorat, INSA de Rennes.

Collet, F., Bart, M., Serres, L., Miriel, J. 2008. Porous structure and water vapour sorption of hemp-based materials. *Constr. Build. Mater*, 22:1271-1280.

Collet, F., Chamoin, J., Pretot S., Lanos, C. 2013. Comparison of the hygric behaviour of three hemp concretes, Energy and Buildings, 62:p. 294-303.

Da SilvaCarla F. P., Chetas, R., Daniel, M., Andy, D., Ansell Martin, P., Ball Richard, J. Influence of eco-materials on indoor air quality, *Green Materials*, 2016, 4:2, 72-80, 2016.

Gourlay, E., Glé, P., Marceau, S., Foy, C., Moscardelli, S. (2017). Effect of water content on the acoustical and thermal properties of hemp concretes, *Constr. Build. Mater.*, **139**, 513-523.

Gunschera. J., Mentese. S., Salthammer, T., Andersen. J. R. Impact of building materials on indoor formaldehyde levels: Effect of ceiling tiles, mineral fiber insulation and gypsum board, *Building and Environment*, 64 (2013), 138-145.

Hameury, S. 2005. Moisture buffering capacity of heavy timber structures directly exposed to an indoor climate: a numerical study. Building and Environment, 40(10), 1400-1412.

Huang, H. and Haghighat, F. Modelling of volatile organic compounds emission from dry building materials. *Building and Environment*, 37 (2002),1127 – 1138.

Koivula, M., Kymäläinen, H.-R., Virta J., et al. 2005. Emissions from thermal insulations--part 2: evaluation of emissions from organic and inorganic insulations, *Building and Environment*, 40:803–814.

Lagouin, M., Magniont, C., Sénéchal, P., Moonen, P., Aubert, J-E, Aurélie- préneron, L. 2019. Influence of types of binder and plant aggregates on hygrothermal and mechanical properties of vegetal concretes, *Construction and Building Materials*, 222:852-871.

Latif, E., Lawrence, M., Shea, A., Walker, P. 2015. Moisture buffer potential of experimental wall assemblies incorporating formulated hemp-lime. *Building and Environment*, 93 (2), 199-209, 2015.

Lelievre, D. 2015. Simulation numérique des transferts de chaleur et d'humidité dans une paroi multicouche de bâtiment en matériaux biosourcés. Université Bretagne-Sud.

Li, X., Wang, S., Du, G., Wu, Z., Meng, Y. (2013). Variation in physical and mechanical properties of hemp stalk fibers along height of stem. Industrial Crops and Products 42,344-348.

Li, X., Xiao,R., Morrell, J. J., Zhou X., and Du, G.(2017). Improving the performance of hemp hurd/polypropylene composites using pectinase pre-treatments. *Ind. Crop. Prod* **97**, 465–468, https://doi.org/10.1016/j.indcrop.2016.12.061.

Luikov, A.V. 1966. Heat and Mass Transfer in Capillary-Porous Bodies. Pergamon, Oxford.

Magniont, C., Escadeillas, G., Coutand M., Oms-Multon, C. 2012. Use of plant aggregates in building ecomaterials, *Eur. J. Environ. Civil Eng*. 16, s17.

Maskell, D., Da Silva, CF., Mower, K., Cheta, R., Dengel, A., Ball, R., Ansell, M., Walker, P., Shea, A. 2015. Properties of bio-based insulation materials and their potential impact on indoor air quality. *First International Conference on Bio-based Building Materials*, 2015.

Mendonça, K.C., Inard, C., Wurtz, E., Winkelmann, F.C., Allard, F. A zonal model for predicting simultaneous heat and moisture transfer in buildings. Indoor Air 2002, 9th International Conference on Indoor Air Quality and Climate (2002).

Moujalled, B., Oumeziane, Y A ., Moissette, S., Bart, M., Lanos, C., Samri, D. 2018. Experimental and numerical evaluation of the hygrothermal performance of a hemp lime concrete building: A long term case study. *Building and Environment*, 136: 11-27. DOI : 10.1016/j.buildenv.2018.03.025.

Nguyen, T. T., Picandet, V., Amziane, S., Baley, C., Influence of compactness and hemp hurd characteristics on the mechanical properties of lime and hemp concrete. European Journal of Environmental and Civil Engineering, 13(9) (2009), 1039-1050

Philip, J.R., De Vries., D.A. Moisture movement in porous materials under temperature gradients. *Transaction of American Geophysical Union* 1957; 38(2): 222-232.

Promis, G., Dutra, LF., Douzane, O., Tran Le, A.D., Langlet T. 2019. Temperature-dependent sorption models for mass transfer throughout bio-based building materials, *Construction and Building Materials*, 197:513-525.

Rahim, M., Douzane, O., Tran Le, A. D., Promis, G.,Laidoudi, B., Crigny A. et al. 2015. Characterization of flax lime and hemp lime concretes: hygric properties and moisture buffer capacity, *Energy Build,* 88: 91–99.

Rode, C., Grunewald, J., Liu, L., Qin, M., Zhang, J. 2020. Models for residential indoor pollution loads due to material emissions under dynamic temperature and humidity conditions, NBS conference, 2020.

Rode, C., Grunewald, J., Liu, L., Qin, M., Zhang, J. Models for residential indoor pollution loads due to material emissions under dynamic temperature and humidity conditions, *NBS conference*, 2020.

Salonvaara, M., Zhang, J. S., Yang, M. A study of Air, Water and VOC Transport Through Building Materials with the Dual Chamber System, in Proc. of Int. Specialty Conf.: *Indoor Environmental Quality – Problems, Research and Solutions, Durham*, NC 2006.

Salonvaara. M., Zhang. J. S., Yang. M. A study of Air, Water and VOC Transport Through Building Materials with the Dual Chamber System, in Proc. of Int. Specialty Conf.: *Indoor Environmental Quality – Problems, Research and Solutions*, Durham, NC 2006.

Samri, D. 2006. Analyse physique et caractérisation hygrothermique des matériaux de construction : approche expérimentale et modélisation numérique, *Thèse ENTPE de Lyon*, France.

Sowell, E.F., and Haves, P. Efficient solution strategies for building energy system simulation. *Energy and Buildings*, 33(2001): 309-317.

Tran le, A D., Maalouf, C., Mendonça, K C., Mai, T.H., Wurtz ,E. Study of moisture transfer in doubled-layered wall with imperfect thermal and hydraulic contact resistances. *Journal of Building Performance Simulation*, 2009(2): 251-266.

Tran Le, A. D., Maalouf, C., Mai, T. H., Wurtz, E., Collet, F.2010. Transient hygrothermal behaviour of a hemp concrete building envelope, *Energy Build*, 42:1797–1806.

Tran Le, A.D., Maalouf, C., Douzane, O., Promis, G., Mai, T.H., Langlet, T. Impact of combined the moisture buffering capacity of a hemp concrete building envelope and interior objects on the hygrothermal comfort in a building, *Journal of Building Performance Simulation*, 9(6):589-605, 2016.

Tran Le, A.D., Nguyen, S. T., Langlet, T.2019. A novel anisotropic analytical model for effective thermal conductivity tensor of dry lime-hemp concrete with preferred spatial distributions, *Energy and Buildings*, 182:75-87.

Viel, M., Collet, F., Lecieux, Y., François, M L M., Colson V., Lanos, C., Hussain, A., Lawrence, M. 2019. Resistance to mold development assessment of bio-based building materials, *Composites Part B: Engineering*, 158, 406-418.

Walker, R., Pavía, S. 2014. Moisture transfer and thermal properties of hemp–lime concretes, *Construction and Building Materials*, Volume 64:270-276.

White. FM., Heat and mass transfer. New York: Addison-Wesley, 1991.

Williams, J., Lawrence, M., Walker, P. 2017. The influence of the casting process on the internal structure and physical properties of hemp-lime. Materials and Structures, 50(2), 108.

Woloszyn, M., Kalamees, T., Abadie, M O., Steeman, M., Kalagasidis, A. S.2009. The effect of combining a relative-humidity-sensitive ventilation system with the moisture-buffering capacity of materials on indoor climate and energy efficiency of buildings. *Building and Environment*, 44: 515 – 524.

Wurtz, E., Haghighat, F., Mora, L., Mendonca, K.C., Maalouf, C., Zhao, H., Bourdoukan, P. 2006. An integrated zonal model to predict transient indoor humidity distribution. ASHRAE *Transactions,* 112(2):175-186.

Xu , Jing., Zhang , J S.2011. An experimental study of relative humidity effect on VOCs' effective diffusion coefficient and partition coefficient in a porous medium, *Building and Environment*, 46 (9):1785-1796.

Xu J, Zhang J, Grunewald J, Zhao J, Plagge R, Amiri Q, et al. A Study on the Similarities between Water Vapor and VOC Diffusion in Porous Media by a Dual Chamber Method. *Clean-Soil, Air, Water* 2009;37 (6),444-453.

Yang, X., Chen Q., Zhang, J. S., Magee, R., Zeng J., Shaw, C. Y.2001. Numerical simulation of VOC emissions from dry materials. *Building and Environment*, 36(10): 1099-1107.

Zhang, J.S. 2005. Combined Heat, Air, Moisture, and Pollutants Transport in Building Environmental Systems. *JSME International Journal*, Series B, 48(2),1-9.

Mendes, N. 1997. Models for prediction of heat and moisturetransfer through porous building elements, Ph.D. Thesis, 225p, Federal University of Santa Catarina,UFSC, Brazil, 1997.